Design and experiment of ground jujube picker based on bionic mechanism

Weijun Wang[1†], Zefeng Liu[1†], Eli·rusul [1*], Bangbang Chen[1], Xiyan Song[1], Dongya Song[1], Hang Yang[1], Peng Zhang[1], Chenghao Wang[2]

(1. *Xinjiang Institute of Technology, School of Mechanical and Electrical Engineering, Akesu 843000, Xinjiang, China*; 2. *Xinjiang Mingyang Mining Construction Group Co., Ltd., Changji 831199, Xinjiang, China*)

Abstract: For mechanized picking of ground jujube under thick planting mode, there arise such issues as ease of damage and inefficient and difficult separation from impurities. In view of this, a bionic arm ground jujube picker was designed on the basis of analyzing jujube planting mode and characteristics, the structural parameters of its key components were determined, and a characteristic model for airflow in the internal flow field of the cleaning system and a movement trajectory model of the gathering device were established. A quadratic orthogonal center composite test was carried out to establish the regression models between influencing factors and the performance of the picker, and analyze the influence law of these factors on the picker. In this test, ground jujubes were taken as the picking object; the forward speed of the picker, the fan speed, and the height of the picking mouth from the ground were taken as the influencing factors; and the picking rate and the impurity rate were taken as the performance indices of the picker. The optimal combination of parameters was determined by multi-objective optimization (MOD): the forward speed of the picker was 0.47 m/s, the fan speed was 3025.76 r/min, and the height of the picking mouth from the ground was 84.20 mm. At this time, the picking rate of the picker was 94.00%, and the impurity rate was 2.30%. According to test verification, the test results and optimization results were consistent, meeting the requirements of mechanized picking of ground jujube.

Keywords: jujube picker, Fluent simulation, test design, cleaning system

DOI: 10.25165/j.ijabe.20251802.8915

Citation: Wang W J, Liu Z F, Eli·rusul, Chen B B, Song X Y, Song D Y, et al. Design and experiment of ground jujube picker based on bionic mechanism. Int J Agric & Biol Eng, 2025; 18(2): 35–44.

1 Introduction

There is a long history of planting jujube in China, and there are many kinds of jujube with high nutritional value, containing a large number of vitamins and mineral elements, enjoying the reputation of "natural vitamins"[1-4]. Xinjiang is suitable for the growth of jujube due to its abundant sunlight, large diurnal temperature variation, and long frost-free period[5]. By the end of 2020, the output of jujubes in Xinjiang amounted to 3.8124 Mt, accounting for about 50% of the total domestic output, making it the main producing area of jujubes in China. The harvest of jujube in Xinjiang is mainly based on mechanical vibration and artificial picking. Both ways require artificial picking when some jujubes fall to the ground during the maturity period, resulting in high labor costs. Also, it overlaps with the harvesting period of maize and cotton, resulting in a large amount of wastage and recovery difficulties. These factors all seriously restrict the rapid development of the jujube industry in Xinjiang[6,7]. Based on this, it is of great value and significance to study a ground jujube picking machine.

There are not many studies on jujube harvesting machinery in foreign countries[8], as jujube is planted in fewer areas abroad, and it is only planted in small quantities in a few countries such as South Korea and Japan. Lee (Chungnam National University, South Korea) explored a fully hydraulic self-propelled jujube harvester based on canopy vibration, which provides little reference as the Korean jujube planting pattern differs greatly from the dwarfing and dense planting pattern in Xinjiang, China[9]. Churchill used a scraper conveying method to accomplish citrus harvesting. However, this machinery has high requirements for ground flatness and easily causes missed picking and fruit damage, and it is mainly used to pick fruits with hard peels[10]. Therefore, the bulky fruit harvesting machinery in foreign countries is not suitable for the harvesting of jujube in the dwarf planting pattern in China.

In China, there is a larger jujube planting area, so the research on jujube harvesting has gone further. Li et al.[11] designed a sweeping-air suction jujube picker, featuring a disc-type sweeping device, which has a small operating area and low efficiency when harvesting jujube. Fu Wei applied a vertical double drum vibration picking device, which separates jujube and branches based on the vibration principle. The advantage is that the jujube harvester straddles the jujube tree to harvest the jujube at one time. However, its weaknesses include poor stability after being raised, damage to

Received date: 2024-03-10 **Accepted date:** 2024-11-03

Biographies: Weijun Wang, Master's degree, Lecturer, research interest: vehicle stability, agricultural machinery, Email: 2022041@xjit.edu.cn; **Zefeng Liu**, MS, Lecturer, research interest: agricultural machinery, Email: 2021034@xjit.edu.cn; **Bangbang Chen**, PhD, Associate Professor, research interest: agricultural machinery, Email: 2018132@xjit.edu.cn; **Xiyan Song**, MS, Lecturer, research interest: agricultural machinery, Email: 2022198@xjit.edu.cn; **Dongya Song**, MS, Associate Professor, research interest: agricultural machinery, Email: 2023023@xjit.edu.cn; **Hang Yang**, MS, Lecturer, research interest: agricultural machinery, Email: 2022193@xjit.edu.cn; **Peng Zhang**, Email: 2021086@xjit.edu.cn; **Chenghao Wang**, BS, Engineer, research interest: agricultural machinery, Email: 1979711728@qq.com.

†The authors contributed same to the work.

***Corresponding author: Eli·rusul**, S, Lecturer, research interest: agricultural machinery. Xinjiang Institute of Technology, School of Mechanical and Electrical Engineering, Akesu 843000, Xinjiang, China Tel: +86-13209939450, Email: 2016093@xjit.edu.cn.

the jujube tree due to the characteristics of machine harvesting, and inability to pick jujube which has fallen on the ground[12]. Ding et al.[13] optimized the vibration frequency of the vibration device in order to improve the vibration harvesting efficiency of the jujube picker, established the kinetic model of the vibration system and jujube tree, and obtained the following parameters: 2.7 rad/s for angle of rotation of the vibration device and 16.9 Hz for vibration frequency. Then, they carried out ADAMS kinematics simulation, which showed that the jujube picking rate reached more than 90% when the motor speed was 25.0-26.5 r/min and the vibration frequency was 16.5-17.4 Hz; the damage rate of jujubes in the harvesting process was less than 8%. It has the advantage of shaking off jujube by the optimal excitation frequency, thus reducing the damage to the jujube tree; its disadvantage is that the rigid connection between the device and the jujube tree causes damage to both the machine and the tree bark, and inability to pick jujube on the ground[13]. Fu et al.[14] established the double-pendulum vibration model of jujube "branch-stalk-fruit" according to the change of instantaneous acceleration in the vibration process, analyzed the intrinsic frequency of system vibration, and carried out the frequency scanning test using the vibration test system. They found that the resonance frequency of jujube trees was concentrated in the range of 12-24 Hz; according to relevant tests and calculations, the maximum instantaneous inertia force of jujube was greater than the maximum tensile force of the stalk, which was 6 N. The test showed that the force transmission effect was good in the process of vibration harvesting at 7 mm amplitude and 17 Hz frequency. The cleaning system is the main device of the jujube picker for the purpose of efficiently separating jujubes and impurities. It is determined through pre-tests that the forward speed of the machine is 0.3-0.6 m/s, the fan speed is 2900-3100 r/min, and the airflow velocity of the cleaning system is 32 m/s[15,16].

Accordingly, there is an urgent need to develop a ground jujube picking machine for dwarf and thick planting mode in Xinjiang, and to promote the mechanization of jujube harvesting. Therefore, a ground jujube picker combining pneumatic and mechanical mode was designed, which adopts a human-like arm to gather ground jujubes into strips, and then collects them in pneumatic mode. It can effectively separate broken soil, twigs, and leaves through secondary screening.

2 Overall structure and working principles

2.1 Overall structure

Figure 1 shows the structure of the ground jujube picker based on bionic mechanism, which combines pneumatic and mechanical mode. It is mainly composed of a frame, gathering device, pick-up unit, collection device, cleaning system, wind power system, and transmission system, among others.

2.2 Working principles

When the jujube picker is working, the negative-pressure airflow formed by the centrifugal fan running at the air inlet is transmitted to the picking mouth through the air duct and the jujube screening box, where the jujubes and impurities are separated; then, the jujubes are discharged from the bottom of the box and transferred to the collection box by the conveyor belt. When the jujubes enter into the collection box from the top of the conveyor belt, the air discharged from the air outlet will be used to clean the remaining jujube leaves in the jujube screening box for the second cleaning of impurities (mainly jujube leaves), thus accomplishing the picking and cleaning of the jujubes.

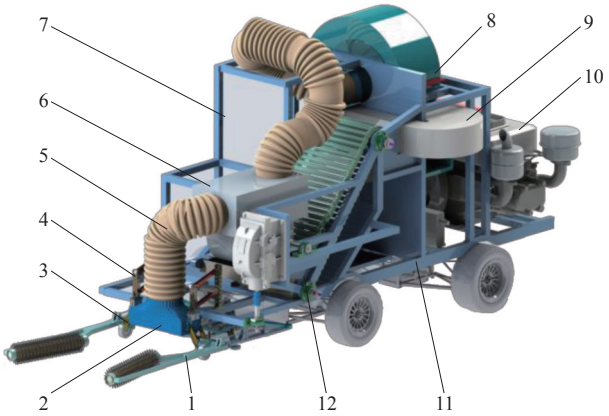

1. Gathering device 2. Air suction picking mouth 3. Feeler mechanism 4. Vibration damping mechanism 5. Rubber duct 6. Jujube screening box 7. Collection box 8. Fan 9. Wind control device 10. Diesel engine 11. Frame 12. Screening mechanism

Figure 1 Overall structure of ground jujube picker

2.3 Working principle of the cleaning system

The cleaning system has the functions of selecting jujubes and impurities, separating impurities and air, and it is the key working part of pickers combining pneumatic and mechanical mode. Its structure diagram and physical drawing are shown in Figures 2 and 3, composed of jujube screening box inlet, filter screen, deflector, impurity air-lock valve and jujube air-lock valve, and jujube outlet, among others. The deflector is located between the jujube screening box inlet and filter screen of the cleaning system, which is used to change the motion characteristics of air in the cleaning system. When the cleaning system is working, the impurity air-lock valve and the jujube air-lock valve can discharge jujubes and impurities in real time, while maintaining the airtightness of the cleaning system.

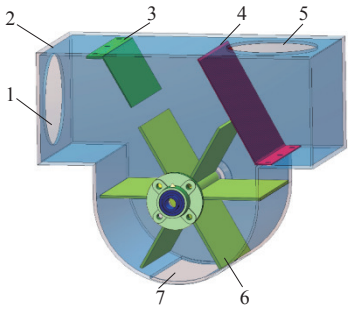

1. Jujube screening box inlet 2. Jujube screening box body 3. Deflector 4. Filter screen 5. Jujube screening box outlet 6. Impurity air-lock valve and jujube air-lock valve 7. Jujube outlet

Figure 2 Structure diagram of jujube screening box in the cleaning system

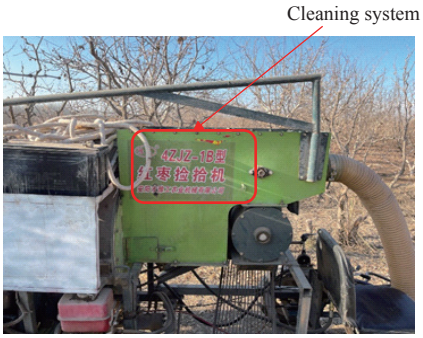

Figure 3 Physical drawing of cleaning system

When the system is in operation, jujubes and impurities enter into the jujube screening box inlet of the cleaning system under the action of negative-pressure airflow. Due to the joint action of the impurity air-lock valve and the filter screen, the airflow trajectory in the cleaning system is changed; under the action of aerodynamics and the filter screen, jujubes settle in the cleaning system, and then they are discharged from the cleaning system through the jujube air-lock valve, and then fall on the conveyor belt, which transports the jujubes into the collection box. Under the action of aerodynamics and the filter screen, one part of the impurities is directly carried out through the airflow over the filter screen, and the other part is blocked by the filter screen, and then discharged from the cleaning system through the impurity air-lock valve, thus accomplishing the cleaning of jujube and impurities.

2.3.1 Cleaning system

In order to improve the effect of jujube settlement and impurity screening, the airflow velocity in the cleaning system should be greater than that of the impurities but less than that of jujube suspension. Therefore, the relevant structural parameters of the cleaning system can be designed according to the airflow velocity in the system. In the area of cleaning system, the Mach number of air is much less than 1, so air can be considered as an incompressible fluid[17]. At the same time, the exchange and leakage of air between the air-lock valve in the cleaning system and the external environment are ignored.

According to the previous studies[18,19] and the working parameters of the picker matched with the ground jujube screening system based on bionic mechanism, it is known that the air velocity at the inlet of the cleaning system is 27-45 m/s, the suspension speed of jujube is 17.2-21.4 m/s, and the suspension speeds of jujube leaves and branches are 0.5-2.2 m/s and 1.2-3.2 m/s, respectively. In order to bring impurities out of the cleaning system, the average air velocity in the system should be greater than 3.2 m/s.

2.3.2 Determination of curve equation of deflector

Some jujubes that enter the cleaning system from the air inlet of the jujube screening box have larger or smaller resistance compared with impurities, so it is difficult for them to settle. Therefore, these jujubes directly collide with the filter screen at the outlet, which will cause further damage to them[20,21], and even lead to deformed jujubes getting caught in the filter screen, which will reduce the working efficiency of the cleaning system and affect the sale of jujubes. Therefore, the deflector is designed between the air inlet of the jujube screening box and the filter screen, and the incomplete elastic collision between the deflector and the jujubes changes their trajectory, which makes the jujubes settle quickly. According to the theorem of momentum and impulse, the smaller the change of velocity direction when jujubes collide with the deflector, the more beneficial it is for jujube damage reduction. Also, the secondary damage caused by the collision of jujubes with the filter screen after crossing the deflector is avoided, and the minimum speed change direction is that the jujubes collide with the deflector and converge on the track at the top of the impurity air-lock valve and the jujube air-lock valve. Shi et al.[15] determined mathematically that the shape of the deflector is an elliptic curve, so the deflector curve presents an angle with the horizontal plane.

In order to analyze the elliptic equation and inclination angle of the deflector surface, the coordinate system OXY is established with the center position of the air inlet of the jujube screening box as the coordinate origin $O(0,0)$, the X-axis parallel to and the Y-axis perpendicular to the air inlet of the jujube screening box. The schematic diagram of the elliptic curve equation of the deflector is shown in Figure 4. At any point $M(x_i,y_i)$, the elliptic curve equation is established as follows:

$$\frac{x^2}{a^2}+\frac{y^2}{b^2}=1 \tag{1}$$

$$\begin{cases} a^2=\dfrac{1}{4}\left(\sqrt{(x_{c1}-x_i)^2+(y_{c1}-y_i)^2}+\sqrt{(x_{c2}-x_{c1})^2+(y_{c2}-y_{c1})^2}\right)^2 \\ b^2=\dfrac{1}{4}((x_{c1}-x_i)^2+(y_{c1}-y_i)^2-(x_{c2}-x_{c1})^2+(y_{c2}-y_{c1})^2) \end{cases} \tag{2}$$

$$\frac{\left(x_i\cos\theta-y_i\sin\theta-\dfrac{\sqrt{(x_{c2}-x_{c1})^2+(y_{c2}-y_{c1})^2}}{2}\right)^2}{a^2}+\frac{(y_i\cos\theta-x_i\sin\theta)^2}{b^2}=1 \tag{3}$$

where, a and b are respectively the length of the major and minor semi-axis of the ellipse, m; θ is the included angle between the elliptic equation and the horizontal plane, (°).

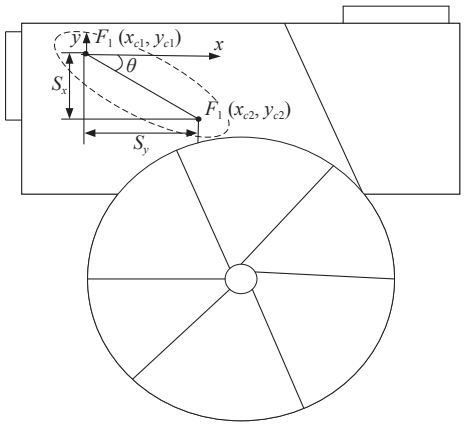

Figure 4 Schematic diagram of deflector curve

In the coordinate system established, the coordinate of F_1 (x_{c1}, y_{c1}) is (0, 0), the projected length of the inlet from the top of the impurity air-lock valve and the jujube air-lock valve on the X-axis is designed as 0.25 m, and y_{c2}=0.25tanθ. By substituting the above values into Equation (3), the simplified deflector equation is as follows:

$$\frac{(4x_i\cos\theta-4y_i\sin\theta-0.25)^2}{\sqrt{x_i^2+y_i^2}-\sqrt{0.25^2+(0.25\tan\theta)^2}}+\frac{4(x_i\sin\theta-y_i\cos\theta)}{x_i^2+y_i^2-\left[0.25^2+(0.25\tan\theta)^2\right]}=1 \tag{4}$$

$$\theta=\arctan\frac{s_y}{s_x} \tag{5}$$

According to the physical knowledge, ignoring the action of airflow except the drag force, jujube makes a quasi-projection motion after entering the cleaning system. The tangent equation of jujube trajectory is established:[22]

$$\begin{cases} a_i=\dfrac{\mathrm{d}v}{\mathrm{d}t} \\ m_ia=\sin\gamma m_ig+F_i \end{cases} \tag{6}$$

where, a_i is jujube acceleration, m/s²; v is jujube speed, m/s; m_i is mass of jujube, kg; g is acceleration of gravity, m/s²; t is time, s; γ is the included angle between the movement direction of jujube i and the horizontal direction, (°). F_i is the drag force on jujubes (N), which is calculated as follows:[4]

$$F_i = \frac{C_i}{8}\rho_{\text{air}}\left|\cos\gamma v_{\text{air}} - v_i\right|(\cos\gamma v_{\text{air}} - v_i)(\pi d_i^2) \tag{7}$$

$$C_i = \begin{cases} \dfrac{24}{Re_p}, & (1 \le Re_p) \\ \dfrac{24(1+0.15Re_p^{0.687})}{Re_p}, & (1 < Re_p < 10^3) \\ 0.44, & (Re_p > 10^3) \end{cases} \tag{8}$$

where, ρ_{air} is air density, here taken as 1.205 kg/m^3; v_{air} is airflow rate, m/s; d_i is projection diameter of the jujube perpendicular to relative velocity direction, m; C_i is flow resistance coefficient (determined by Reynolds number of particles)[23,24]. Re_p is Reynolds number obtained by introducing porosity.

$$Re_p = \frac{\varepsilon\rho_{\text{air}}|\mu_{\text{air}} - v_i|d_i}{v_{\text{air}}} \tag{9}$$

where, ε is porosity, %; μ_{air} is air dynamic viscosity, here taken as 14.8×10^{-6} m^2/s. According to the simultaneous Equations (8) and (9), the calculated Reynolds number is greater than 10^3, which belongs to the turbulence model. By substituting c_i = 0.44 into (7) and associating (6) yields, we can get the following:

$$F_i = 0.055\left|\cos\gamma v_{\text{air}} - v_i\right|(\cos\gamma v_{\text{air}} - v_i)(\pi d_i^2) \tag{10}$$

According to the jujube motion trajectory equation:

Trajectory equation in the horizontal direction:

$$s_x = v_0 t + \frac{1}{2}\frac{\cos\gamma F_i}{m_i}t^2 \tag{11}$$

Trajectory equation in the vertical direction:

$$s_y = \frac{1}{2}\left(\frac{\sin\gamma F_i}{m_i} + g\right)t^2 \tag{12}$$

where, v_0 is the initial velocity of jujube, m/s.

The test shows that when jujube enters the cleaning system, the maximum initial velocity is 6.5 m/s, and θ=9.43° according to Equations (9)-(11); that is, the angle between the deflector and the horizontal plane is 9.43°.

2.3.3 Modeling and simulation analysis of cleaning system

The cleaning system model built in Solidworks2021 is transformed into parasolid.x_t format, then imported into ANSYS/mech module for grid division and saved as .msh format, and then imported into ANSYS/Fluent module for simulated calculation. The inlet airflow velocity is set to 40 m/s, and the outlet velocity is set to 30 m/s. The key simulation parameters are set as listed in Table 1.

Table 1 Fluent simulation settings

Parameter	Option	Parameter	Option
Calculation pattern	Three-dimensional double precision	Velocity and pressure coupling	SIMPLE
Solver	Pressure-based solver	Element gradient interpolation method	Least squares cell-based
Solving model	VOF model	Discretization scheme of pressure modification coefficient	Body force weighted
Viscosity model	Standard k-ε turbulence model	Initialization	Mixed initialization
Flow model	Transient flow	Time step	0.0001 s
Discretization scheme of convective term	Second order upwind	Material	Air

In order to study the air motion characteristics in the cleaning system, Fluent 2022 software was used to simulate and analyze the internal flow field of the cleaning system, and the results are shown in Figure 5.

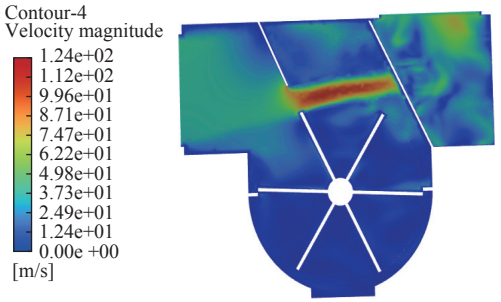

a. Cloud diagram of airflow velocity

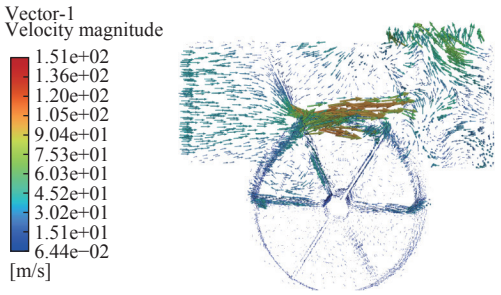

b. Vector diagram of airflow velocity

Figure 5 Fluid simulation analysis results of the cleaning system

Figure 5a is the cloud diagram of airflow velocity in the cleaning system. It can be seen that the airflow velocity increases first and then decreases after entering the cleaning system, which is beneficial for the settlement of jujube. A high airflow zone is formed between the lower part of the deflector and the filter screen, which is beneficial for the airflow to carry light impurities across the impurity air-lock valve and jujube air-lock valve. Figure 5b is the vector diagram of airflow velocity in the cleaning system; the airflow trajectory changes at the front and lower ends of the deflector, the impurity air-lock valve, and the jujube air-lock valve, which can effectively guide the jujubes to settle. The airflow gathers below the deflector and changes sharply, which is more conducive to carrying impurities across the top ends of the impurity air-lock valve and the jujube air-lock valve. A small amount of impurities enter into the impurity air-lock valve and jujube air-lock valve due to the obstruction of jujube. Under the effect of the specific gravity difference between jujube and impurity, some impurities are removed through the impurity air-lock valve, and the other part is rotated by the impurity air-lock valve and jujube air-lock valve and carried with a straight filter screen, and is then removed through the filter screen, thus accomplishing secondary cleaning. The simulation results of the flow field in the cleaning system show that the characteristics of airflow motion in the system meet the expected results.

3 Design of key components and determination of suspension speed of jujubes

3.1 Gathering device

3.1.1 Analysis of gathering conditions

The gathering device functions by simulating the action of manually gathering jujubes. As shown in Figure 6, the scattered jujubes are aligned into strips by hands and arms under the reciprocating swing, thus gathering jujubes on the ground. In this gathering process, as shown in Figure 7, jujube is thrown up and aligned under the combined action of transverse and longitudinal force, which should meet the following conditions:

$$F_y + F_N \geq G \tag{13}$$

$$F_x - f_s > 0 \tag{14}$$

$$F = \frac{F_x}{\cos\alpha} \tag{15}$$

where, F is the toggle power for dates, N; F_s is the friction between jujube and ground, N; α is the angle between point of force on jujube and horizontal plane, (°).

According to the analysis and statistics of jujube characteristics in the early stage, the average gravity G of super-grade jujube is 5 g each, the ground friction is 10 N, and the friction factor μ is 0.02.

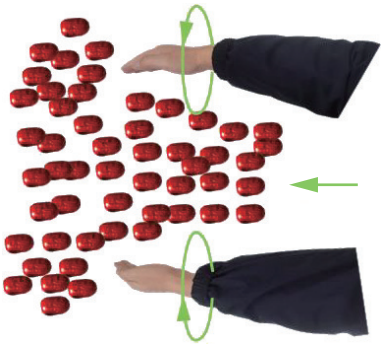

Figure 6 Manual gathering of jujubes

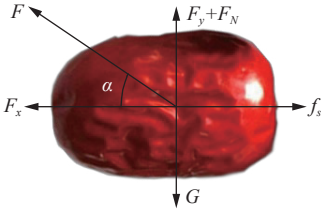

Figure 7 Jujube force model

3.1.2 Design of gathering device

According to the working principle of human-like arm gathering, jujube rolls to the left and right and goes up and down in the gathering process. The left-right rolling of jujube is realized by a crank-rocker mechanism, and the up-and-down fluctuation is realized by a rotating rubber roller with hydraulic drive. The principle of the gathering device is shown in Figure 8.

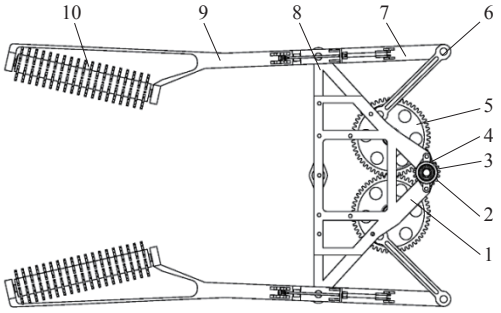

1. Upper bracket 2. Gear 3. Gear shaft 4. Bearing seat 5. Gear 6. Connecting rod 7. Rocker rod 8. Lower bracket 9. Swing arm rocker 10. Rotating rubber roller

Figure 8 Principle of gathering device

3.1.3 Design of jujube gathering left-right rolling mechanism

The schematic diagram of the left-right rolling mechanism for gathering jujubes is shown in Figure 9. According to the overall structural design, arrangement, and gathering working range, the following parameters can be determined: swing angle $\psi = 27.5°$; minimum transmission angle $\gamma_{min} = 40°$, and travel velocity-ratio coefficient K=1.26. According to the mechanical principles, the relational expression of travel velocity-ratio coefficient in planar four-bar linkage is obtained:

$$\theta = 180\frac{K-1}{K+1} \tag{16}$$

where, θ is the included angle between extreme positions of the crank-rocker mechanism ABCD, (°).

According to △ACD, △AC_1D, and △ACC_1 in Figure 9, by using the triangle cosine theorem, we can get the following:

$$\begin{cases} (l_1+l_2)^2 = l_3^2 + l_4^2 - 2l_3l_4\cos(\theta_1+\psi) \\ (l_2-l_1)^2 = l_3^2 + l_4^2 - 2\cos\theta_1 \\ \left(2l_3\sin\dfrac{\psi}{2}\right)^2 = (l_1+l_2)^2 + (l_2-l_1)^2 - 2(l_1+l_2)(l_2-l_1)\cos\theta \end{cases} \tag{17}$$

where, l_1 is the length of crank AB, mm; l_2 is the length of connecting rod BC, mm; l_3 is the length of rocker rod CD, mm; l_4 is the length of frame AD, mm; θ_1 is the stopping phase angle of rocker rod CD, (°).

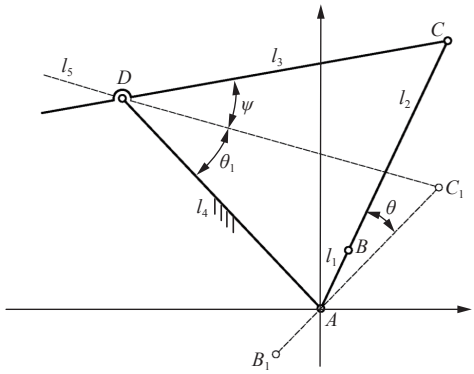

Figure 9 Schematic diagram of jujube gathering left-right rolling mechanism

According to the existence condition of crank in the crank-rocker mechanism and the calculation relationship of minimum transmission angle γ_{min}, we can get the following:

$$l_1 + l_3 \leq l_2 + l_4 \tag{18}$$

$$\cos\gamma_{min} = \frac{l_2^2 + l_3^2 - (l_4 - l_1)^2}{2l_2l_3} \tag{19}$$

The travel velocity-ratio coefficient K and rocker swing angle ψ have been determined, and the length of frame does not affect the movement speed of rocker CD. Considering the space installation position of AD, set l_4=300 mm, and substitute $\gamma_{min} = 40°$ and $\psi = 27.5°$ into Equations (4)-(7) to obtain the parameters of crank-rocker mechanism: l_1=70 mm, l_2=250 mm, and l_3=350 mm.

3.1.4 Design of rotating rubber roller

The rotating rubber roller mainly realizes the action of lifting of human-like arm, and is used in conjunction with the swing arm rocker to gather jujubes from the ground. Its structural feature is that the rubber strip is uniformly fixed on the rotating thin-walled cylinder, and jujubes on the ground are aligned clockwise according to the direction of manual driving and the forward speed of the machine (as shown in Figure 10).

3.2 Modeling and simulation analysis of gathering device

3.2.1 Modeling and simulation

In our design, the model is built based on SolidWorks2021 three-dimensional software. According to the previous theoretical research and the design of overall transmission scheme, the virtual assembly and interference check of the parts are carried out, and the

structural parameters of the interference parts are modified. The model is saved in .x_t format, and simulated by ADAMS mechanical system kinematics and dynamics simulation software. This simulation mainly analyzes the matching problem of swing arm rocker speed, rotating rubber roller speed, and machine forward speed, and the verification of human-like arm trajectory. According to the working principle of the gathering device, the constraint relationship of actual motion is added to all parts, and the sliding pair is added to the whole device and the ground to better control the simulated forward speed. Because the device is a symmetrical structure, only one side is taken for motion simulation, as shown in Figure 11.

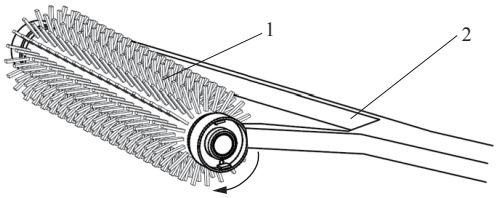

1. Rotating rubber roller 2. Swing arm rocker

Figure 10 Structure of rotating rubber roller

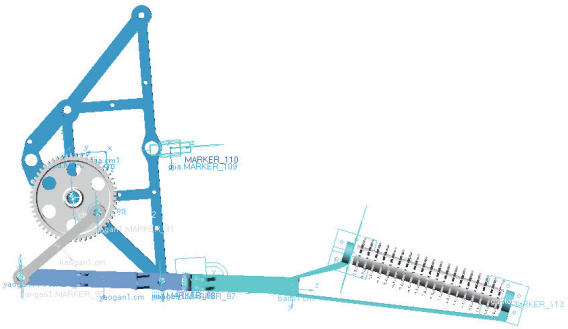

Figure 11 Structure of rotating rubber roller

3.2.2 Simulation results

According to the working principle and motion characteristics, the simulation end time is 4 s and the simulation steps are 1000, and the motion trajectory of the end of the gathering device is shown in Figure 12. As can be seen from Figure 12a, the maximum spreading displacement S_{max}=0.606 m, the minimum spreading displacement S_{min}=0.133 m, the half working range of the gathering device is S=S_{max} – S_{min}=0.473 m, and the total working range is 0.946 m, which meets the design requirements. As can be seen from Figure 12b, the trajectory point on the rotating rubber roller in the gathering device moves in an elliptical shape in the vertical space, which conforms to the trajectory of human hands moving up and down in the process of gathering jujubes, and realizes the movement of human hands gathering jujubes. As can be seen from Figure 12c, in the process of gathering jujubes, the contact speed of jujubes changes from small to large and then back to small, and there is no sudden change, which reduces the damage to jujubes caused by the rotating rubber roller and meets the working requirements of gathering jujubes and the performance requirements of the device itself.

3.3 Determination of jujube suspension speed

When jujubes are sucked up by negative pressure formed by the picker, they are suspended in the airflow and remain relatively static with the ground, and the airflow velocity at this time is the suspension speed of jujubes. According to the stress analysis of jujubes, they are subjected to gravity, attractive force, and air resistance, so the critical suspension speed of jujube is as follows:[25]

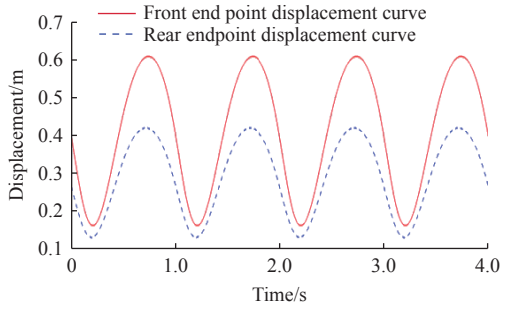

a. Left-right gathering trajectory

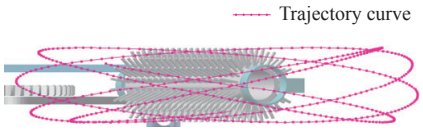

b. Up-and-down motion trajectory

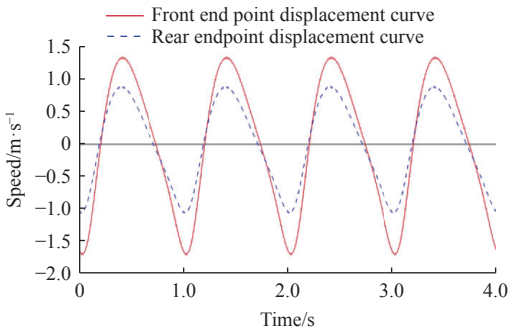

c. Speed curve diagram

Figure 12 Gathering device simulation diagram

$$\begin{cases} v_{critical} = \sqrt{\dfrac{8m_{max}g - 2\pi g\rho_{air}xy^2}{\pi C_d \rho_{air} y^2}} \\ v = K \cdot v_{critical} \end{cases} \quad (20)$$

where, C_d is resistance constant; ρ_{air} is air density, kg/m^3; x is the minor axis diameter of jujube, m; y is the major axis diameter of jujube, m; $v_{critical}$ is the theoretical airflow velocity, m/s; v is the actual airflow velocity, m/s; m_{max} is the maximum mass of jujube, kg; g is the acceleration of gravity, m/s^2; and K is the reliability constant of jujube suction.

In order to reduce the error caused by factors such as shape and size of jujube and collision, the range of K is 1.8-2.0, and K=2. According to the suspension characteristics and experiments of jujube[26-28], the critical suspension speed of jujube is determined to be 20.94 m/s, and the actual airflow velocity is finally determined to be greater than 30 m/s taking into account the influence of various factors on jujube suspension.

4 Overall test

4.1 Test conditions

The performance test of the jujube picker was carried out on October 28, 2023, in Group 2, Brigade 8 of Yixilaimuqi Township, Wensu County, Akesu Prefecture. The test area was 300 m long and 32 m wide, where jujube trees were spaced by 4 m, the average spacing of the plants was 2 m, and the variety was grey jujube, with a moisture content of 31.05%. The main test was the performance test of the cleaning system, as shown in Figure 13.

4.2 Test method

According to research from Zhang et al.[25], it was found that when the forward speed of the jujube picker is higher than 0.7 m/s, not all jujubes on the ground can be picked up, which makes it

a. Before picking b. After picking

Figure 13 Jujube test site

difficult to screen jujubes and impurities, and the picking efficiency is even lower when the forward speed is lower than 0.3 m/s. When the fan speed is higher than 3100 r/min, a large number of jujubes are picked up in a short time, which causes accumulation of a large number of jujubes in the cleaning system, thus making it difficult to separate jujubes from impurities. When the fan speed is lower than 2900 r/min, the cleaning system has poor working performance and poor picking effect. According to the pre-tests, the airflow velocity is the key factor to determine the separation and picking efficiency of jujubes and impurities. In the field work, the optimal working state of the jujube picker is determined by the separation effect of jujubes and impurities. Therefore, it is determined that the airflow rate is adjusted by the speed of variable frequency fan. The fan speed range is 2900-3100 r/min, the airflow rate range is 27-45 m/s, and the forward speed of the picker is 0.3-0.7 m/s. According to DG/T 188-2019 *Fruit Picker*, Q/XNJ 001-2017 *Self-propelled Air Suction Jujube Picker*, and GB/T 5667-2008 *Productive Testing Methods for Agricultural Machinery*, the field test is carried out. Before the test, relevant parameters of the jujube picker are adjusted to meet the test requirements. The test factors are determined, including forward speed of the picker, fan speed, and height of the picking mouth from the ground. The test indices are impurity rate and picking rate, where impurity rate is the ratio of the mass of impurities to that of harvested jujubes, and picking rate is the ratio of the mass of harvested jujubes to that of ground jujubes. The test indices are determined by Equations (21)-(22). The test is repeated for three times, and the result is the arithmetic average.

$$\eta_0 = \frac{\sum_{i=1}^{3} m_0}{\sum_{i=1}^{3} m_{R0} + \sum_{i=1}^{3} m_0} \tag{21}$$

$$\eta_d = \frac{\sum_{i=1}^{3} m_d}{\sum_{i=1}^{3} m_{R0} + \sum_{i=1}^{3} m_d} \tag{22}$$

where, η_0 is impurity rate, (%); m_0 is the mass of impurities discharged from the impurity air-lock valve, kg; m_{R0} is the mass of harvested jujubes, kg; η_d *is* picking rate, (%); m_d is the mass of jujubes discharged from the impurity air-lock valve, kg.

4.3 Test program

In order to investigate the influence law of test factors on the indices, a quadratic orthogonal center composite test was carried out using the Central Composite Design module of the Design-Expert 12 software, with the factor intervals shown in the ranges described in section 3.2 and the test factor level codes listed in Table 2.

4.4 Test results and analysis

According to the theory of Central Composite Design in Design-Expert 12 software, forward speed of picker, fan speed, and height of the picking mouth from the ground are defined as the influencing factors for the response surface test, while impurity rate and picking rate are defined as the response values. The parameters are modified by the quadratic regression orthogonal test program with three factors and five levels. The orthogonal test program and the results are listed in Table 3. The test consists of a total of 20 groups. From the test results, the jujube picker has an impurity rate of 1.7%-9.6% and picking rate of 82.9%-94.5%.

Table 2 Test factor levels

Level	Factor		
	Forward speed/ m·s^{-1}	Fan speed/ r·min^{-1}	Height of picking mouth from the ground x_2/mm
Upper asterisk arm (1.682)	0.67	3099.2	98.82
Upper level (1)	0.6	3060	92
Zero level (0)	0.5	3000	82
Lower level (–1)	0.4	2945	72
Lower asterisk arm (–1.682)	0.33	2905.8	65.18

Table 3 Test program and results

Test code	Influencing factors			Response indicators	
	Forward speed A	Fan speed B	Height of picking mouth from the ground C	Picking rate Q/%	Impurity rate M/%
1	–1	–1	–1	88.8	3.1
2	1	–1	–1	82.9	8.8
3	–1	1	–1	88.7	2.4
4	1	1	–1	88.1	4.1
5	–1	–1	1	88.7	2.0
6	1	–1	1	83.6	8.5
7	–1	1	1	87.3	1.7
8	1	1	1	88.8	4.0
9	–1.68	0	0	86.5	3.0
10	1.68	0	0	82.9	9.6
11	0	–1.68	0	86.8	7.4
12	0	1.68	0	90.8	2.7
13	0	0	–1.68	87.3	3.2
14	0	0	1.68	89.8	2.0
15	0	0	0	94.5	3.2
16	0	0	0	94.3	3.5
17	0	0	0	93.4	2.5
18	0	0	0	93.9	3.3
19	0	0	0	94.2	3.2
20	0	0	0	93.8	3.6

4.4.1 Significance test and regression model

The multiple regression fitting analysis was performed by Design-Expert 12 software according to the test data in Table 3[29-32], a regression model was established for the quadratic response surface of jujube impurity rate and picking rate on the three independent variables (forward speed of the picker, fan speed, and height of the picking mouth from the ground), and an ANOVA was performed, as shown in Equations (23)-(24) and Table 3.

$$Q = 94.01 - 1.18A + 1.14B + 0.3005C + 1.49AB + 0.3625AC - 0.1625BC - 3.26A^2 - 1.81B^2 - 1.9C^2 \tag{23}$$

$$M = 3.23 + 2.00A - 1.33B - 0.3089C - 1.02AB + 0.1750AC + 0.075BC + A^2 + 0.5613B^2 - 0.305C^2 \tag{24}$$

where, Q is jujube picking rate, %; M is impurity rate, %.

According to ANOVA in Table 4, the p value of the model of picking rate and impurity rate of jujube in the response surface model is less than 0.0001 (p<0.01), which indicates that the regression model is highly significant; the p value of the loss of fit

terms is 0.1293 and 0.5714, respectively, which is not significant, indicating that there are no unconsidered factors affecting the test indices; and the coefficients of determination R^2 are 0.9887 and 0.9875, respectively, which indicates that the model can be fit to the test results of 98.87% and 98.75%, respectively. With the above test results, it can be known that the relevant parameters of the machine can be optimized by the model. In the jujube picking rate model, A, B, AB, A^2, and B^2 have highly significant influence on the regression model (p<0.01), while AC and BC have no significant influence on the regression model (p>0.05). In the jujube impurity rate model, A, B, AB, A^2, and B^2 have highly significant influence on the regression model (p<0.01), while AC and BC have no significant influence on the regression model (p>0.05). The optimized equations with the insignificant regression terms removed are shown below.

$$Q = 94.01 - 1.18A + 1.14B + 0.3005C + 1.49AB - 3.26A^2 - 1.81B^2 - 1.9C^2 \quad (25)$$

$$M = 3.23 + 2.00A - 1.33B - 0.3089C - 1.02AB + A^2 + 0.5613B^2 - 0.305C^2 \quad (26)$$

The test of the regression coefficients in Equations (25)-(26) concludes that the primary and secondary factors affecting the picking rate and impurity rate are: forward speed, fan speed, and height of picking mouth from the ground.

4.4.2 Effect analysis of test factors

In the evaluation of jujube picking performance indices, picking rate and impurity rate are key performance indices of the machine. According to the established regression model of picking rate and impurity rate, one of the test factors is set to zero level, and the response surface and contour map are drawn, as shown in Figures 14 and 15.

Table 4 ANOVA of jujube picking rate and impurity rate

Source of variation	Picking rate				Impurity rate			
	Sum of squares	*df*	*F*	*p*	Sum of squares	*df*	*F*	*p*
Model	272.77	9	97.04	<0.0001**	109.10	9	87.83	<0.0001**
A	19.11	1	61.18	<0.0001**	54.57	1	395.42	<0.0001**
B	17.88	1	57.26	<0.0001**	24.00	1	173.90	<0.0001**
C	1.23	1	3.95	0.0118*	1.30	1	9.44	0.0118*
AB	17.70	1	56.68	<0.0001**	8.40	1	60.90	<0.0001**
AC	1.05	1	3.37	0.2123	0.245	1	1.78	0.2123
BC	0.2113	1	0.6764	0.5806	0.045	1	0.3261	0.5806
A^2	153.04	1	490.01	<0.0001**	14.50	1	105.09	<0.0001**
B^2	47.17	1	151.03	0.0002**	4.54	1	32.89	0.0002**
C^2	51.89	1	166.15	0.0109*	1.34	1	9.71	0.0109*
Residual	3.12	10			1.38	10		
Lack of fit residual	2.33	5	2.96	0.1293	0.6318	5	0.8442	0.5714
Pure error	0.7883	5			0.7438	5		
Total	275.89	19			110.48	19		

Note: ** indicates highly significant (p<0.01); * indicates significant (p<0.05)

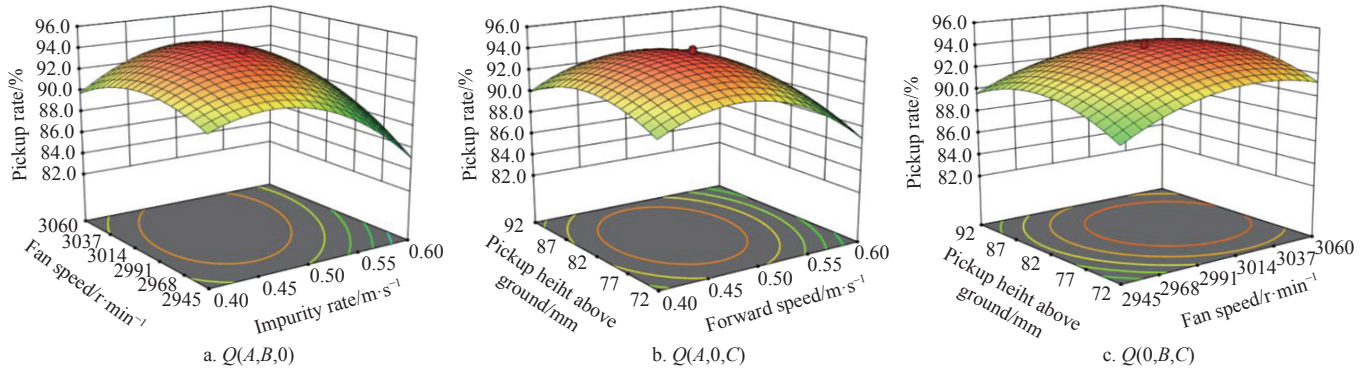

a. $Q(A,B,0)$ b. $Q(A,0,C)$ c. $Q(0,B,C)$

Figure 14 Influence of various factors on picking rate

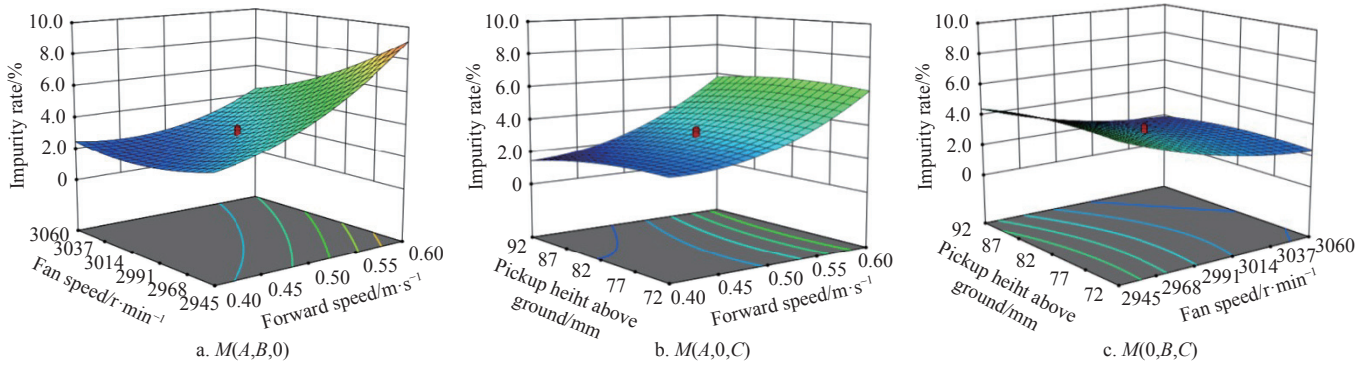

a. $M(A,B,0)$ b. $M(A,0,C)$ c. $M(0,B,C)$

Figure 15 Influence of various factors on impurity rate

As shown in Figures 14a and 15a, when the height of the picking mouth from the ground is at the central level (82 mm), the picking rate first increases and then decreases with the increase of forward speed and fan speed. The impurity rate increases with the increase of forward speed, but decreases with the increase of fan speed. This is because with the increase of forward speed and fan speed, a lot of jujubes and impurities are drawn into the screening system, while the fan speed increases to blow the leaves out of the screening system, increasing the picking rate. When the forward speed and fan speed continue to increase, the machine continues to draw in jujubes and impurities, and the screening system is full, in which case the gap between jujubes and impurities becomes small

and not conducive to separation, and therefore the picking rate becomes smaller. With the increase of fan speed and wind force, leaves and other objects are blown out of the screening system to reduce the impurity content. When the forward speed is low (less than 0.5 m/s), it has little influence on picking rate and impurity rate. When the forward speed is high (>0.5 m/s), it has great influence on picking rate and impurity rate.

As shown in Figures 14b and 15b, when the fan speed B is at the central level (3000 r/min), the picking rate first increases and then decreases with the increase of forward speed and height of picking mouth from the ground, while the impurity rate always increases. This is because as the forward speed and the height of picking mouth from the ground increase, the machine draws a lot of jujubes and impurities into the screening system. The picking rate increases first when the screening system is not full and has the optimal screening efficiency; but when the screening system is full as the machine continues to draw in jujubes and impurities, the gap between them negatively affects the separation, so the picking rate decreases, and the impurity rate increases as leaves and other objects cannot be blown out of the screening system. When the forward speed is low (less than 0.5 m/s), it has little influence on picking rate and impurity rate. When the forward speed is high (greater than 0.5 m/s), it has great influence on picking rate and impurity rate.

As shown in Figures 14c and 15c, when the forward speed is at the central level (0.5 m/s), the picking rate increases first and then decreases with the increase of fan speed and height of picking mouth from the ground, while the impurity rate always decreases. This is because as the fan speed and the height of picking mouth from the ground (picking area) increase, the machine draws a lot of jujubes and impurities into the screening system. The picking rate increases first when the screening system is not full and has the optimal screening efficiency; but when the screening system is full as the machine continues to draw in jujubes and impurities, the gap between them negatively affects the separation, so the picking rate decreases. With the increase of fan speed and wind force, leaves and other objects are blown out of the screening system to reduce the impurity content. When the fan speed is low (less than 3000 r/min), it has a great influence on picking rate and impurity rate. When the fan speed is high (greater than 3000 r/min), it has little influence on picking rate and impurity rate.

4.4.3 Parameter optimization

When the forward speed is 0.4-0.6 m/s, the fan speed is 2945-3060 r/min, and the height of picking mouth from the ground is 72-92 mm, the main objective function method in multiple response is used to optimize the influencing factors, namely forward speed, fan speed, and height of picking mouth from the ground, and picking rate and impurity rate are used as performance index functions for optimization solution. The objective function and constraints are as follows:

$$\begin{cases} \max Q \\ \min M \\ Q > 93\% \\ M < 3\% \\ \text{s.t.} \begin{cases} 0.33 \text{ m/s} \le A \le 0.67 \text{ m/s} \\ 2905.8 \text{ r/min} \le B \le 3099.2 \text{ r/min} \\ 65.18 \text{ mm} \le C \le 98.82 \text{ mm} \end{cases} \end{cases} \tag{27}$$

In order to achieve the optimal working performance of the ground jujube picker, the influencing factors in the test are optimized. For the optimal working parameters of the picker, optimization solution is obtained by Design-Expert 12 data processing software, which results in the optimal parameter combination of the influencing factors: forward speed 0.47 m/s, fan speed 3025.76 r/min, and height of picking mouth from the ground 84.20 mm. The predicted values of the objective function are 94.00% and 2.30% for picking rate and impurity rate, respectively.

4.5 Test verification

In order to verify the optimization results of the working parameters of the jujube picker and the operational performance of the cleaning system, test verification is repeated five times with the above optimal parameter combination, as shown in Figure 16, and the results are the arithmetic average. The test concludes that the average picking rate is 93.7%, which is greater than 93.0%, and the average impurity rate is 2.5%, which is less than 3.0%. It can be seen that the test results and optimization results are consistent, meeting the requirements of mechanized picking of ground jujube.

a. Before field picking test b. After field picking test

Figure 16 Field test

5 Conclusions

(1) According to the requirements for picking up jujube and jujube characteristics, a ground jujube picker was designed, which adopted the air suction method. The parameters of the key components were determined, and relevant calculations were carried out on the suspension speed of jujubes and the gathering device. Also, the key factors affecting the picker performance were defined as follows: forward speed, fan speed, and height of picking mouth from the ground.

(2) The performance of the ground jujube picker based on bionic mechanism in the field was mainly evaluated by two indices, namely picking rate and impurity rate. The main influencing factors for the working indices are forward speed of the picker, fan speed, and height of the picking mouth from the ground. The picker draws in jujubes through the negative pressure airflow formed by centrifugal fan, and carries out the first jujube and impurity separation in the cleaning system, after which the jujubes are transmitted to the collection box through the conveyor belt, and enter into the collection box from the top of the conveyor belt. The remaining jujube leaves in the jujube screening box are cleaned by airflow for secondary cleaning, thus accomplishing the picking and cleaning of jujubes.

(3) The quadratic orthogonal center composite test was performed. The regression model was established between the performance indices of the picker and various test factors, and the influence of these factors on response indicators was analyzed based on the response surface. The optimal combination of working parameters was determined by multi-objective optimization (MOD): forward speed 0.47 m/s, fan speed 3025.76 r/min, and height of picking mouth from the ground 84.20 mm. In this case, the performance indices of the picker are 94.00% for picking rate and 2.30% for impurity rate.

Acknowledgements

This research was funded by Key projects at the university level (ZZ202401), Xinjiang Tianchi Talents" Introduction Programme Funding Project (Letter from the Xinjiang Department of Human Resources and Social Security [2024] No. 57) (2023TCLJ03), and Xinjiang Specialty Food Processing Equipment R&D Centre (PT202104).

[References]

[1] Younis M, Ahmed I A M, Ahmed K A, Yehia H M, Abdelkarim D O, Alhamdan A. The effects of thermal and pulsed electric field processing on the physicochemical and microbial properties of a high-fiber, nutritious beverage from a milk-based date powder. AgriEngineering, 2023; 5(4): 2020–2031.

[2] Li Y P, Zhou X Y, Zhao K L, Liu J C, Chen G H, Zhang Y P, et al. Cultivation and morphology of jujube (*Ziziphus Jujuba* Mill.) in the Qi River Basin of Northern China during the Neolithic Period. Scientific Reports, 2024; 14(1): 2305–2305.

[3] Yao S Q, Shi G K, Wang B S, Peng H J, Meng H W, Kan Z. Calibration of the simulation parameters of jujubes in dwarfing and closer cultivation in Xinjiang during harvest period. Int J Agric & Biol Eng, 2022; 15(2): 256–264.

[4] Bai S H, Yuan Y W, Niu K, Zhou L M, Zhao B, Wei L G, et al. Design and parameters optimization of the curved sieve for an air suction jujube harvester. Int J Agric & Biol Eng, 2024; 17(2): 132–139.

[5] Yang L. Analysis on the dilemma and solutions of emerging economical crops in frontier villages—taking the red jujube crop of K Village in Ruoqiang County as an example. Agricultural Forestry Economics and Management, 2023; 6(4): 59–64.

[6] Zhang X C, Chen B Q, Li J B, Fang X, Zhang C L, Peng S B, et al. Novel method for the visual navigation path detection of jujube harvester autopilot based on image processing. Int J Agric & Biol Eng, 2023; 16(5): 189–197.

[7] Xu H Z, Hua Y, He J, Chen Q L. The positive and negative synergistic airflow-type jujube fruit harvester (P-N JH). Processes, 2022; 10(8): 1486–1486.

[8] Ahmad I, Maryam, Ercisli S, Anjum M A, Ahmad R. Progress in the methods of jujube breeding. Erwerbs-Obstbau, 2023; 65(4): 1217–1225.

[9] Lee S W, Kim D H, Lee C K, Seo S W, Huh Y K. Development of a collecting system for jujube harvester. Journal of Biosystems Engineering, 2006; 31(6): 500–505.

[10] Churchill D B, Summer H R. A new system for raking and picking up oranges. Transaction of the ASAE, 1977; 20(4): 617–620.

[11] Li S F. Design and experimental study on key components of sweep and air suction pick-up jujube harvesting machinery. Xinjiang Agricultural University, 2020. (in Chinese)

[12] Fu W, He R, Qu J L, Sun Y, Wang L H, Kan Z. Design of self-propelled dwarf and close planting jujube harvester. Journal of Agricultural Mechanization Research, 2024; 36(4): 106–109. (in Chinese)

[13] Ding K, Zhang B C, Diao X Y, Zhang H M, Fu W, Kan Z. Optimization and experiment of vibration device shaking frequency of jujube harvester. Journal of Agricultural Mechanization Research, 2019; 41(3): 21–25, 33.

[14] Fu W, Zhang Z Y, Liu Y D, Pan J B, Cui J, Ding K, et al. Simulation experiment in lab on force transfer effect of jujube under vibration excitation. Transactions of the CSAE, 2017; 33(17): 65–72. (in Chinese)

[15] Shi G K, Li J B, Ding L P, Kan Z. Design and experiment of inertia pneumatic type cleaner system of jujube fruit. Transactions of the CSAM, 2022; 53(6): 167–176.

[16] Zhang X J, Bai S H, Jin W, Yuan P P, Yu M J, Yan J S, et al. Development of pneumatic collecting machine of red jujube in dwarfing and close cultivation. Transactions of the CSAE, 2019; 35(12): 1–9. (in Chinese)

[17] Zhao S X, Feng Z. Gas flow characteristics of argon inductively coupled plasma and advections of plasma species under incompressible and compressible flows. Chinese Physics B, 2018; 27(12): 352–364. CNKI: SUN: ZGWL. 0.2018-12-050.

[18] Zhang F K, Yu F S, Li Z J, Zhang H, Lan H P, Li P, Zhang C J. Design and field testing of the air-suction machine for picking up Chinese jujube fruits. Journal of Fruit Science, 2020; 37(2): 278–285. (in Chinese)

[19] Zhang F K, Zhang H, Lan H P, Yu F F, Li Z J, Li P. Simulation analysis of pneumatic conveying device of air-suction jujube picker based on CFD-EDM coupling. Journal of Agricultural Science and Technology, 2021; 23(7): 107–116. (in Chinese)

[20] Li R, Peng J, Sun S, Al-Mallahi A, Fu L S. Determination of selected physical and mechanical properties of Chinese jujube fruit and seed. CIGR e-Journal, 2016; 18(3): 294–300.

[21] Wu L G, He J G, Liu G S, Wang S L, He X G. Detection of common defects on jujube using Vis-NIR and NIR hyperspectral imaging. Postharvest Biology & Technology, 2016; 112: 134–142.

[22] Zewdu A D. Aerodynamic properties of tef grain and straw material. Biosystems Engineering, 2007; 98(3): 304–309.

[23] Liu J, Liu H N. Fluid mechanics. Peking University Press, 2023. (in Chinese)

[24] Ni W J. Computational fluid dynamic. China Machine Press, 2021. (in Chinese)

[25] Zhang X J, Bai S H, Jin W, Yuan P P, Yu M J, Yan J S, Zhang C S. Design and flow simulation of suction chamber of air suction type jujube picking device. Journal of Agricultural Mechanization Research, 2020; 42(8): 91–95. (in Chinese)

[26] China Academy of Agricultural Mechanization, Agricultural machinery design manual. China Machine Press, 2007. (in Chinese)

[27] Xu K C, Wang H Q, Gai J F. Fan Brochure. China Machine Press, 2011. (in Chinese)

[28] Yu F F, Li P, Zhang F K, Li Z J, Zhang H, Fan X W. Experimental determination and analysis of suspension velocity characteristics for red jujube. Journal of Chinese Agricultural Mechanization, 2020; 41(6): 99–105. (in Chinese)

[29] Yan W, Hu Z C, Wu N, Xu H B, You Z Y, Zhou X X. Parameter optimization and experiment for plastic film transport mechanism of shovel screen type plastic film residue collector. Transactions of the CSAE, 2017; 33(1): 17–24. (in Chinese)

[30] Ni X D, Xu G J, Wang Q, Peng X R, Wang J, Hu B. Design and experiment of pneumatic cylinder array precision seed-metering device for cotton. Transactions of the CSAM, 2017; 48(12): 58–67. (in Chinese)

[31] Chen J N, Zhang X W, Liu L M, Ma X X, Yao K, Cheng D. Design and experiments of the clipping-stem type non-circular gear transplanting mechanism for corn pot seedlings. Transactions of the CSAE, 2023; 39(18): 30–40. (in Chinese)

[32] Xie J H, Zhang Y H, Cao S L, Zhang Y, Zhou J B, Meng Q H. Design and experiment of stalk pressing type cotton field mulch film collectors. Transactions of the CSAE, 2023; 39(18): 51–63. (in Chinese)